Uncertainty analysis of a test-rig for centrifugal compressors

Valencia E.*; Granja V.*; Palacios J.*; Poveda R.*; Cando E.; Hidalgo V.****

**Escuela Politécnica Nacional, MechanicalEngineeringFaculty, Quito, Ecuador*
e-mail: {esteban.valencia;jose.palacios; maria.granja;ricardo.povedac}@epn.edu.ec
*** Tsinghua University, Department of Thermal Engineering, Beijing, China*
e-mail: {edgar.cando; victor.hidalgo}@epn.edu.ec

Resumen: El presente trabajo establece el procedimiento experimental llevado a cabo para obtener las curvas características de un compresor, y busca describir el método de propagación de incertidumbres en los resultados finales de un banco de pruebas para compresores centrífugos y de esta forma calibrar la apreciación de la instrumentación y mejorar así su precisión. Se ha desarrollado un método numérico para considerar todas las incertidumbres, errores y factores de calibración de los diferentes instrumentos de medición y procesamiento de información.
Se realiza el análisis de los datos obtenidos experimentalmente y se muestra una comparación entre la gráfica experimental del compresor y la gráfica dada por el fabricante. Adicionalmente, se realiza un análisis de la incertidumbre de los datos experimentales para encontrar los parámetros que interfieren en mayor grado sobre las curvas características del compresor.

Palabras clave: Banco de pruebas, ciclos combinados de potencia y energía,factores de calibración, incertidumbres, microturbinas.

Abstract: This work stablishes the experimental procedure aimed to obtain a compressor performance map, and the description of the uncertainty propagation method in the final results of a test-rig for centrifugal compressors to improve the accuracy and therefore the precision of the experimental set-up. A mathematical method has been developed to implement all the uncertainties, errors and calibration factors of the different measuring and processing devices.
The analysis of the experimental data is performed. A comparison between the experimental compressor map and the original equipment map (OEM) is shown. Additionally, an uncertainty analysis of the experimental data is performed to find the parameters that affect largely the compressor map.

Keywords: Calibration factors, combined heat and power cycles, generation, microturbines, test-rigs, uncertainties

1. INTRODUCTION

The use of boilers for stationary energy production has become common over the years. However, these systems have numerous disadvantages such as maintenance issues, pollution, lower operating efficiencies, large size, among others, allowing more efficient technologies such as microturbinesto take place in the energy production market.

Microturbines designed for Combined Heat and Power (CHP)applications are largely based on off-the-shelf turbomachinery technology, as it provides a critical advantage in terms of costs over competing alternatives. In this study, off-the–shelf turbomachinery works on different conditions for which it was designed. Therefore, this work aims to reproduce as close as possible the operating conditions of the compressor, such that the model obtained of its performance can reliably represent its characteristics. For this, an experimental compressor map based on the experimental data obtained through the TU Delft test-rig has been developed. As the experimental data uses a measuring system that comprises of several components, the uncertainties introduced by these components in the measurements have to be considered. The computation of the influence of error sources such as calibration factors, location errors, random errors, etc. in the results, allows usto determine how good our experimental set-up is, since they indicate the influence of each uncertainty source on the variables of interest.

Uncertainties are important in all sort of experimental procedures and should be considered during the different stages of an experimental program. In the planning phase the analysis of the measurement system, guides the decision-making process for selecting appropriate and cost–effective systems and methodologies, reducing the risk of making wrong decisions.

There are many approaches that can be used to compute uncertainties. However, the two main approaches are given by American Society of Mechanical Engineers (ASME) and by the International Organization for Standardization (ISO).

Valencia E., Head of Fluids and Turbomachinery Laboratory, Assistant Professor of Mechanical Engineering Department, EPN, Ph.D. candidate at Cranfield University.
Granja V., Assistant Professor of Mechanical Engineering Department, EPN.
Palacios J., Head of Thermodynamics Laboratory, Assistant Professor of Mechanical Engineering Department, EPN.
Poveda R., Assistant Professor of Mechanical Engineering Department, EPN.
CandoE., Assistant Professor of Mechanical Engineering Department, EPN, Ph.D. candidate at Tsinghua University.
HidalgoV., Associate Professor of Mechanical Engineering Department, EPN, Ph.D. candidate at Tsinghua University.

Based on the standards issued by these two organizations a scheme is selected to compute the range of uncertainties for the parameters of interest.

To analyze the behavior of the compressor its experimental performance map is drawn. For this, the equations and procedure to compute the necessary parameters are developed. Analogously a scheme to calculate the uncertainties of the parameters of interest based on the uncertainties of the measured parameters is developed. The literature that treats uncertainty calculation use the term "final result'' to indicate the parameters of interest which in the current case are pressure ratio, efficiency, corrected rotational speed and corrected mass flow.

In the current case the final results depend on the measured variables, which present their uncertainties in catalogues. A propagation uncertainty method is used to obtain the uncertainties of the final results. This method of propagation is based on the norm ASME PTC 19.1.
Norms and literature about uncertainties suggest two methods to carry out the propagation of uncertainties. Those schemes are the Taylor series method (TSM) and the Monte Carlo method (MCM).

The characteristics that present the TSM are:

- The data available from catalogues can be used directly and the calculation of each uncertainty component (systematic and random) can be performed separately.
- This method for the case of the systematic uncertainty calculation does not need repeated measurements to get a sample population, so it is less time consuming.
- Since this method calculates the uncertainty in the final results based on the sensitivity factors of each measured value, it makes easier the uncertainty analysis.

The characteristics that present the MCM are:

- As currently developed the Labviewmodel, it delivers only average values which produce a small sample population while testing. Therefore, to achieve a significant sample population the number of tests has to be very large making this method very time consuming.
- This method takes advantage of the high computing speed available nowadays.
- Since the true value of the measured parameters is unknown, the calculation of the systematic uncertainty needs special attention in this case.

For these reasons, in this work the TSM method is selected for the uncertainties propagation and the scheme presented in the norm ASME PTC 19.1 is used.

After selecting the scheme to be used to deal with the uncertainties, the results are obtained and the uncertainties are analyzed such that only the principal uncertainty sources can be selected. Due to the large amount of time that the sampling process to calculate the random uncertaintytakes, its contribution in the total uncertainty is analyzed. The comparison shows a small influence of this component in the final uncertainty (for static pressure, temperature and mass flow), then using the rule of thumb presented in [9]its contribution is neglected in further calculations. In this work the only parameter which presents both uncertainty components is the corrected speed, where both uncertainty components present comparable magnitudes.

1.1 CHP cycle

Microturbines operate on the principle of the Brayton cycle and comprises of a compressor, turbine, combustion chamber andrecuperator as shown in Fig.1.
Heat production is achieved with the use of a heat recovery system located after the recuperator and the electricity is produced by an electrical generator coupled to the shaft of the microturbine.

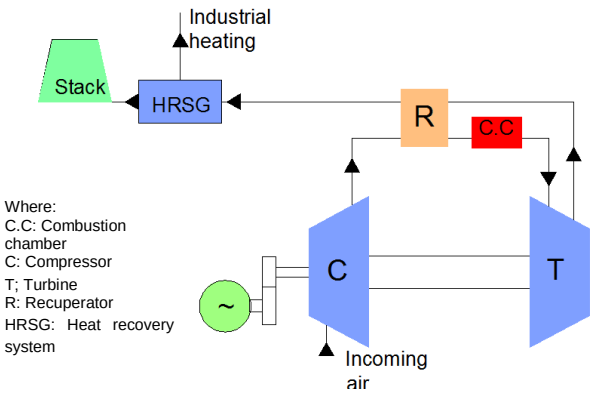

Figure 1. Schematic view of amicroturbine system

The working principle is the same as a normal gas turbine. There are three stages that continuously produce energy: compression, combustion and expansion.

Some of the general performance parameters for the analysis are shown in Table 1.

Table 1. Conceptual design study assumptions for ISA performance and efficiencies [12]

Parameter	Unit	Value
Air flow	[g/s]	35-45
Thermal power	[kW]	Simple cycle: 35-45/ Recuperated: 10-18
η_{is_c}	[%]	70
N	[rpm]	240000
PR_c	[-]	2,4
TIT	[K]	1300
η_{is_t}	[%]	65
η_{cc}	[%]	99,5
η_{mech}	[%]	97

1.2 Test-rig

The test-rig has the aim of testing the compressor in conditions as close as possible to the ones at which it performs in the microturbine framework. It comprises of measurement equipment and tested equipment. It was mounted according to the norms SAE J1723 and SAE J1826. In Fig. 2 the main components of the TU Delft test-rig are shown.

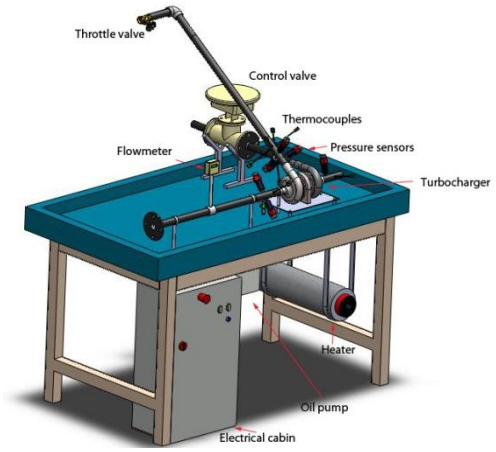

Figure 2.A three dimensional view of the test-rig with its parts

1.2.1 Instrumentation

They measure the thermodynamic parameters and convert them in electrical signals. In the following subsections the sensors used in the test-rig and their characteristics are presented. The tables 2, 3,4,5,6, 7 and 8are assembled such that the scheme presented in Fig. 3 can be followed.

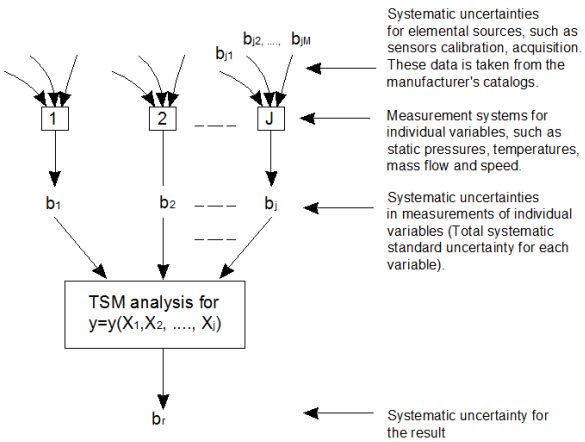

Figure 3. Systematic uncertainty calculation for the final results [9]

a) Thermocouples

A thermocouple operates on the basis of the junction located in the process producing a small voltage difference which increases with temperature. The location and number of thermocouples are based in norms SAE J1723 and SAE J1826.

The test-rig uses nine thermocouples of two different ranges, and they are distributed in the following way: two at the compressor inlet, four at the compressor outlet, two at the turbine inlet and one at the turbine outlet.

Table 2. Systematic uncertainties for the thermocouples at each station [5, 6, and 11]

Error source	$B_{\bar{x}i}\,(°K)$	$b_{\bar{x}}$	$B_{\overline{x_O}}\,(°K)$	$b_{\overline{x_O}}$
Calibration	1.5	0.75	0.4 % R. or 1.5	0.2 % R. or 0.75

Notes:

(1) Whichever value is greater

b) Pressure sensors

The pressure sensors used at the compressor outlet have larger full scale. The pressure sensors have a full scale of 0,6 MPa. at the inlet stations, and 0,8 MPa. at the outlet stations.

Table 3. Systematic uncertainties for the pressure sensors at each station [1]

Error source	$B_{\bar{x}i}$	$b_{\bar{x}i}$	$B_{\overline{x_O}}$	$b_{\overline{x_O}}$
Calibration	0.5 % F.S.	0.25% F.S	0.5% F.S	0.25% F.S.

Notes:

(1) This value includes accuracy and linearity error

c) Flowmeter

This is an inmersible mass flowmeter for gas flow measurement applications. A thermal sensor controls the calibration of the device.

Table 4. Systematic uncertainties for the flowmeter [2]

Error source	$B_{\bar{x}}(g/s)$	$b_{\bar{x}}$
Calibration	0.5% F.S.±1% R	0.25 %F.S.± 0.5% R
Repeatability	0,2% FS.	0,1% FS.

Notes:

(1) The full scale used is 100 g/s.

d) Speed sensor

The method used for measuring the revolution speed in the turbocharger is a system called PicoTurn [8].

Table 5. Systematic and random uncertainties for the speed sensor [8]

Error source	$B_{\bar{x}}$(mV)	$b_{\bar{x}}$	$S_{\bar{x}}$	$s_{\bar{x}}$
Calibration	±3	±1.5 mV	±0.25% F.S.	±0.125 % F.S.

Notes:

(1) The calibration factor given by the manufacturer is 80 krpm/V.
(2) The full scale is 320000 rpm.

e) *Acquisition system*

The acquisition system collects the signals produced by each sensor and send them to the computer. There are different modules for each sensor. The modules are located on the chassis NI cDAQ 9172 [3, 4].

Table 6. Systematic uncertainties for the pressure transducer module Ni 9203 [4]

Error source	Pressure transducer Ni 9203 [12]	
	$B_{\bar{x}}$ (mA)	$b_{\bar{x}}$ (mA)
Calibration	±0.04%R±0.02%FS.	±0.02%R±0.01%FS.

Notes:

(1) The values are for a typical calibration (25 ^{0}C±5^{0}C)
(2) The transducer used is unipolar and is used for the flowmeter as well
(3) The calibration factors are 0,3 bar/mA and 0.4 bar/mA for pressure at inlet and outlet stations respectively and 5g/s/mA for mass flow
(4) The sampling rate is 200 kS/s max or 16 bits

Table 7. Systematic uncertainties for the rotational speed module, Ni 9201 [4]

Error source	$B_{\bar{x}}$(V)	$b_{\bar{x}}$ (V)
Calibration	±0.04%R±0.07%FS	±0.02%R±0.035%FS.

Notes:

(1) The values are for a typical calibration
(2) The calibration factor is 32 krpm/V
(3) Sampling rate 500kS/s or 12 bit

Table 8. Systematic uncertainties for the thermocouple module at each station [4, 11]

Error source	$B_{\bar{x}}$ (°C)	$b_{\bar{x}}$ (^{0}C)
Calibration	1.3	0.65.

Notes:

(1) This is the typical error for a NI 9211 module when a type K thermocouple is used. The error takes into account: gain error, offset error, differential and integral non linearity noise errors and isothermal errors. The values are for a typical calibration with a range of temperatures from 0-100 ^{0}C
(2) Sampling rate is 14 S/s or 24 bits

The test-rig configuration is based on norms and the equipment has been installed such that the required data to draw a compressor map can be collected in a reliable and systematical way. In Fig.4 the process of data collection is shown.

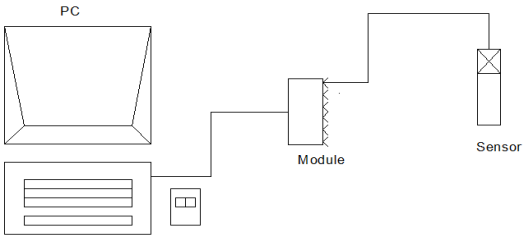

Figure 4. Process of data collection

2. METHODOLOGY

2.1Uncertainties

The total error of a measurement comprises of the systematic (bias) and the random portion. Fig. 5 shows the total error components.

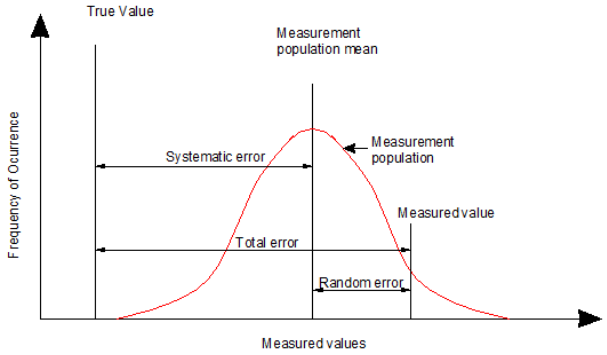

Figure 5. Components of total error [7]

The random error is the portion of the total error that varies randomly in repeated measurements during a test. The sources of this error are of random nature which arises from uncontrolled test conditions and non-repeatability in the measurement system [7].

Systematic error is the portion that remains constant in the measurements during a test [7].

In Table 9 a classifications for the random and systematic error components can be observed. This classification was used to interpret the data established by the manufacturers.

Table 9. Classification of manufacturing's data in terms of elemental errors [10]

Error	Error Type
Accuracy	Systematic
Common-mode voltage	Systematic
Hysteresis	Systematic
Installation	Systematic
Linearity	Systematic
Loading	Systematic
Spatial variation	Systematic
Noise	Random
Repeatability	Random
Resolution/scale	Random
Thermal stability	Random
Quantization	Random

2.3 Approaches for uncertainty calculation

While the estimation of the individual uncertainty is based on widely accepted statistical concepts, there are several methods that can be utilized to determine how individual sources of uncertainty are propagated to obtain the uncertainty at the final result. The approach selected for this paper is established by the norm ASME PTC 19.1 and is called ''test of uncertainty''.

This norm standardizes the process of calculation and is also worldwide applied. The latter standards (2005) harmonized their original methodologies developed in 1970s and 1980s withGUM (1993)method by adding assumptions necessary to achieve a less complex "large" samplemethodology required by GUM and retaining the use of traditional engineering concepts of systematic (bias) and precision (random) uncertainties.

2.3.1 Random uncertainty

If an infinite number of samples are taken, the population mean (μ), the standard deviation (σ), and the frequency distribution of the population can be determined.
Since an infinite number of samples is not realistic, in the current case the population values have to be changed to a sample values. Then, all the previous definitions can be developed in function of these sample values. The sample mean is given by:

$$\bar{X} = \frac{\sum_{j=1}^{N} X_j}{N}, \qquad (1)$$

WhereX_j is the value of each is sample and N is the number of samples.

The sample standard deviation is given by:

$$s_x = \sqrt{\sum_{j=1}^{N} \frac{(X_j - \bar{X})^2}{N-1}}. \qquad (2)$$

Since the sample mean is just an estimate of the population mean there is an inherent error, then the sample mean can be used to define the probable interval where the population mean with a certain confidence level is expected [7]. Then the random standard uncertainty is related to the sample standard deviation as follows:

$$s_{\bar{x}} = \frac{s_x}{\sqrt{N}} \qquad (3)$$

This concept comes from the fact that it is not sufficient to know the uncertainty value but also it is necessary to know the probability that it can occur. The random expanded standard uncertainty for a 95% of confidence is given by:

$$S_{\bar{x}} = 2\, s_{\bar{x}} \qquad (4)$$

2.3.1 Systematic uncertainty

For the current test the systematic uncertainty is provided by the manufacturers of the measuring instruments. This published information does not present an interval of confidence, so it is assumed that the population of data has a normal distribution within a 95% of confidence. This recommendation is based on the large number of tests that the manufacturers carry out to calibrate their instruments [8]. With this assumption the elemental systematic uncertainty is given by:

$$b_{\overline{xk}} = \frac{B_{\overline{xk}}}{2}, \qquad (5)$$

Where$B_{\overline{xk}}$ is the systematic standard expanded uncertainty.

2.3.2 Summation of uncertainties

As several parameters (total temperature, static pressure, mass flow and rotational speed) are measured, there are several sources of systematic and random uncertainty for each one of the parameters. These uncertainty components should be summed for each measured parameter, such that only one total uncertainty for each measured parameter can be calculated. Bearing in mind this aspect the random and systematic uncertainty are given by:

$$\begin{aligned} s_{\bar{x}} &= \left(s_{\bar{x}_1}{}^2 + s_{\bar{x}_2}{}^2 + s_{\bar{x}_3}{}^2 + \cdots\right)^{1/2} \\ &= \left(\sum_{i=1}^{j} s_{\bar{x}_i}{}^2\right)^{1/2} \end{aligned} \qquad (6)$$

$$\begin{aligned} b_{\bar{x}} &= (b_{\bar{x}_1}{}^2 + b_{\bar{x}_2}{}^2 + b_{\bar{x}_3}{}^2 + \cdots)^{1/2} \\ &= \left(\sum_{i=1}^{j} b_{\bar{x}_i}{}^2\right)^{1/2} \end{aligned} \qquad (7)$$

The number of components (*j*) appears since for the measurement of each variable a couple of devices are used. Equation 0 is not useful in the most of cases, because the random component is not always indicated in the catalogues of each component. To get around to this problem, the total random uncertainty is calculated directly through repeated sampling (7) takes the systematic error contribution of each component used in the measurement of each variable. This equation is used in the present work since the systematic uncertainties are given in the device catalogues.

2.3.2 Propagation of uncertainties

Since the variables of interest to draw the compressor map (efficiency, pressure ratio, corrected mass flow and corrected speed) can not be directly measured, their uncertainties can not be determined from catalogues or other sources. Therefore, it is necessary to calculate them based on the uncertainties of the measured values. Some methods have been developed to solve this problem and the theory behind all this procedures is called propagation of uncertainty [7].

Taylor Series Method (TSM)

This method needs the variable with the unknown uncertainty expressed in function of the other variables of known uncertainty. In the current case, all the variables calculated can be expressed in explicit functions of the measured variables. The explicit function in terms of its variables can be expanded with the Taylor formula in the following way:

$$y = f(X_1, X_2, X_3, ..),$$

$$y = f(\bar{x}) = f(\overline{x_0}) + \left(\frac{\partial f}{\partial X_1}(\overline{x_0}) + \frac{\partial f}{\partial X_2}(\overline{x_0}) + \frac{\partial f}{\partial X_3}(\overline{x_0}) + \cdots\right).(\bar{x} - \overline{x_0}) \quad (8)$$

Due to the suitability that presents this method to compute the systematic and random uncertainties, based on the existing relations between the variables measured and calculated, this method is used in the present case. Applying the procedure analogously for a multiple variable function, the second part of (8) can be rewritten in the following way:

$$\delta_y = \theta_{x1}.\delta_1 + \theta_{x2}.\delta_2 + \theta_{x3}.\delta_3 + \cdots \quad (9)$$

Using this latter for our uncertainties, we get for the propagation of uncertainty the following:

$$b_y = \left(\sum_{i=1}^{j}(\theta_{xi}\, b_i)^2\right)^{1/2}, \quad (10)$$

$$s_y = \left(\sum_{i=1}^{j}(\theta_{xi}\, s_i)^2\right)^{1/2}, \quad (11)$$

Finally the sum of uncertainties is given by

$$u_{\bar{x}} = \sqrt{{b_{\bar{x}}}^2 + {s_{\bar{x}}}^2}. \quad (12)$$

For the current case, it is assumed a normal distribution for which a confidence level of 95% can be achieved with a student's factor (t) of 2 [7]. The total expanded uncertainty is given by:

$$U_{\bar{x}} = t\, u_{\bar{x}} \quad (13)$$

2.3.2 Uncertainty analysis

Uncertainty Analysis is a useful tool for all phases of a measurement program from initial planning to detailed design, debugging, testing operational procedures and data analysis. The first factor is called uncertainty magnification factor (UMF) and is defined as the factor which for a given variable X_i indicates the influence of the uncertainty of that variable on the uncertainty in the result. It is given by:

$$UMF_i = \frac{X_i}{y}\frac{\partial y}{\partial X_i} \quad (14)$$

Where(X_i) represents the variables and (y) represents the function result. For the current case X_i is : P_2, P_3, T_{2o}, T_{3o}, ṁ and y is: *PR,* η,$\dot{m}_c$,N_c. A UMF value greater than 1 indicates that the influence of the uncertainty in the variable is magnified as it propagates through the data reduction equation into the result.

Another useful parameter is the uncertainty percentage contribution (UPC). This provides for a given X_i the percentage contribution of the uncertainty in that variable to the squared uncertainty in the result. Since the UPC of a variable contains effects of both the UMF and the magnitude of the uncertainty of the variable, it is useful in the planning phase once we begin to make estimates of the uncertainties of the variables[9].

3. RESULTS

In Table 10 the deviation percentages of the systematic and random uncertainties for the pressure ratio and efficiency are presented.

Table 10. Percentage of deviation of systematic and random uncertainties

N [krpm]	ṁ [g/s]	Deviation $b_{\bar{x}}$ [%]		Deviation $s_{\bar{x}}$ [%]	
		PR	η	PR	η
120	40	1.871	8.630	0.0415	0.194
	50	1.941	12.396	0.0273	0.240
160	40	1.746	4.700	0.0405	0.214
	50	1.787	5.422	0.0515	0.472
190	40	1.664	3.271	0.0526	0.172
	50	1.679	3.440	0.0527	0.240

Notes:

(1) Due to the complexity to fix the same mass flow for both cases, the values for the comparison correspond to similar mass flow values in the range of ± 2 g/s.

(2) The deviation has been determined by $\%\,deviation = \frac{U_x}{X+U_x} \times 100$, where U_x is the uncertainty in the test point and X is the corresponding variable measured.

(3) Since the number of samples in the case of the random uncertainty does not allow to assume a normal distribution, for this comparison has been used the total uncertainties of both uncertainty components without a range of confidence.

As observed in Table 10 the total systematic uncertainty is two orders of magnitude larger than its random counterpart. Thus the total combined uncertainty depends more on the systematic portion than on the random one. The latter component can be neglected due to its small contribution. In the same way that the random component is small for the pressure ratio and efficiency, the corrected mass flow also presents the same pattern.

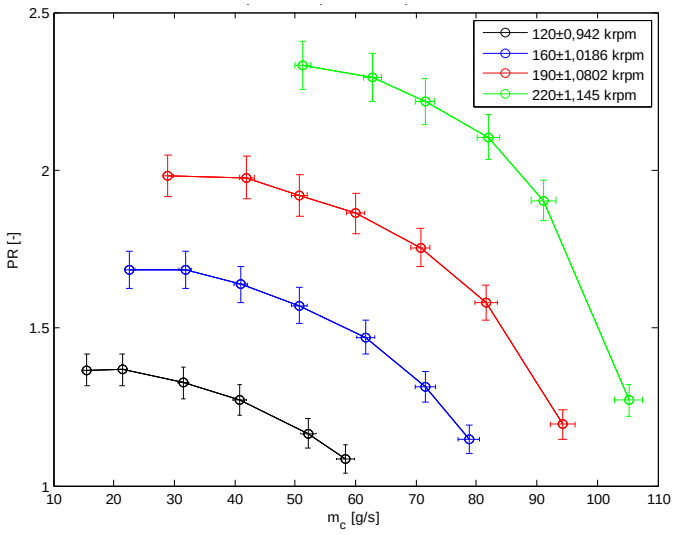

Figure 6. Compressor map with uncertainties in terms of pressure ratio.

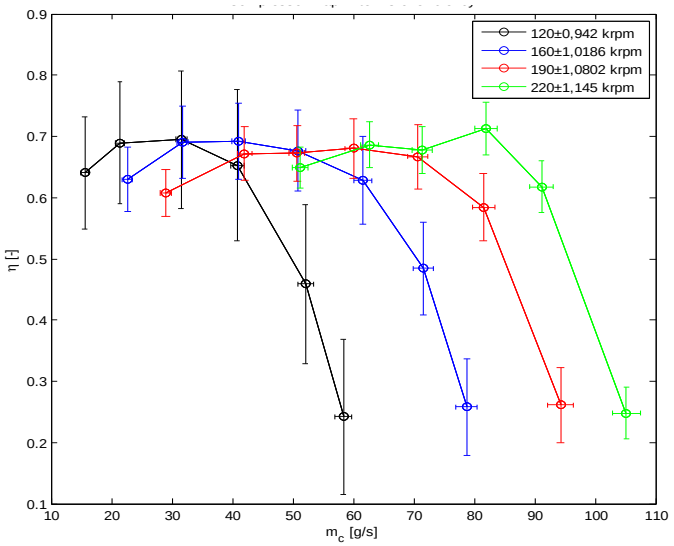

Figure 7. Compressor map with uncertainties in terms of efficiency.

Fig.6 and Fig. 7 show the compressor maps with their corresponding uncertainties which are presented as bars for each operating condition. The uncertainties for pressure ratio, efficiency and corrected mass flow are based only on the systematic component.

The uncertainty for the corrected speed is based on random and systematic components and it corresponds to the average of the uncertainty values at different operating points at certain speed.

4. DISCUSSION OF RESULTS

Table 11 and Table 12 show the UMFs and UPCs of the measured parameters for different mass flows at 120, 160 and 190 krpm. It was decided do not use the data at 220 krpm, since at that speed the measuring process can not be carried out continuously for the whole speed-line, which means that the measured values are not reliable enough for this analysis. Moreover, it is sufficient to compare the factors at the three different speeds to figure out the trend presented by the factors.

According to the UMFs values for the pressure ratio, the influence of the uncertainties due to the static pressure at inlet and outlet stations of the compressor does not increment during the uncertainty propagation, since these two variables have values near to 1. The UMFs corresponding to the other variables are smaller than 1, which indicates that the influence of their uncertainties decrease when they are propagated.

The UPCs for the pressure ratio show that its uncertainty has a large dependence on the static pressures uncertainties, which is logical since the pressure ratio should be more influenced by these two parameters. In this case the UPCs show that a special attention requires the uncertainty of the pressure sensors, since they contribute in large extent to the pressure ratio uncertainty.

The UMFs for the efficiency show that the influence of the uncertainties for the static pressure and total temperatures at the outlet and inlet station of the compressor increase when they are propagated, since they are larger than 1. Due to this aspect the uncertainties presented in Fig. 7 (efficiency diagram) are larger than the ones presented in Fig.6 (pressure ratio).

It can be also observed that the UPCs for the efficiency show good agreement with their corresponding UMFs for all the variables, being notorious the large influence of the static pressure uncertainties in the efficiency uncertainty. Moreover there is an increment of the temperature uncertainty contribution for the efficiency uncertainty when the speed is increased. This last aspect makes that the uncertainty bars in Fig.7 become smaller at higher speeds, since the thermocouple uncertainties produce smaller uncertainties in the efficiency than the pressure uncertainties.

Table 11. UMFs and UPC for pressure ratio at different mass flows

$\dot{m}$ [g/s]	N [krpm]	PR									
		UMF_{P_2}	UPC_{P_2}	UMF_{P_3}	UPC_{P_3}	$UMF_{T_{o2}}$ 1E-03	$UPC_{T_{o2}}$ 1E-5	$UMF_{T_{03}}$ 1E-03	$UPC_{T_{o3}}$ 1E-5	$UMF_{\dot{m}}$ 1E-3	$UPC_{\dot{m}}$ 1E-4
40	120	1,004	57,631	1,004	42,369	2,23	1,45	1,81	0,787	0,849	0,179
50		1,003	61,780	1,002	38,220	1,37	0,59	0,944	0,227	0,856	0,254
60		1,002	63,746	1,001	36,254	0,821	0,219	0,524	0,710	0,593	0,171
40	160	1,004	71,209	1,002	28,790	2,11	1,62	1,04	0,269	2,15	1,47
50		1,003	72,859	1,001	27,141	1,39	0,713	0,634	0,100	1,51	0,923
60		1,002	73,966	1,001	26,034	0,839	0,264	0,365	0,329	0,948	0,497
40	190	1,004	78,699	1,002	21,301	2,11	1,78	0,754	0,136	2,72	2,59
50		1,003	79,630	1,001	20,370	1,46	0,857	0,496	0,0591	1,93	1,60
60		1,001	79,712	1,000	20,288	0,695	0,196	0,240	0,0137	0,909	0,558

Table 12. UMFs and UPC for efficiency at different mass flows

$\dot{m}$ [kg/s]	N [krpm]	η									
		UMF_{P_2}	UPC_{P_2}	UMF_{P_3}	UPC_{P_3}	$UMF_{T_{o2}}$	$UPC_{T_{o2}}$	$UMF_{T_{o3}}$	$UPC_{T_{o3}}$	$UMF_{\dot{m}}$ 1E-3	$UPC_{\dot{m}}$ 1E-4
40	120	6,688	50,039	6,682	36,787	11,244	7,201	11,241	5,972	5,65	0,156
50		4,326	46,883	4,322	29,003	10,207	13,299	10,205	10,815	3,69	0,193
60		3,696	46,568	3,694	26,484	9,281	15,006	9,280	11,942	2,19	0,125
40	160	2,368	51,420	2,363	20,790	5,914	16,448	5,912	11,342	5,08	1,06
50		2,179	51,757	2,176	19,280	5,575	17,313	5,574	11,650	3,28	0,656
60		2,065	52,473	2,063	18,469	5,293	17,532	5,292	11,527	1,95	0,353
40	190	1,687	55,587	1,682	15,045	4,285	18,338	4,283	11,030	4,57	1,83
50		1,620	56,086	1,617	14,347	4,129	18,521	4,127	11,046	3,11	1,13
60		1,611	58,574	1,610	14,908	3,815	16,736	3,815	9,782	1,46	0,410

6. CONCLUSIONS AND RECOMMENDATIONS

The methodology shown in this paper could be used in further experimental set-ups where the uncertainty of the instrumentation is known. Additionally, the uncertainty analysis method could give us a good overview of the quality of our experimental set-up.

The present work deals with the procedure to obtain the performance map of the TU Delft test-rig centrifugal compressor and compare its performance with the data presented by the OEM.

It has been used the norm ASME PTC 19.1 as a guideline for the uncertainty calculation. Using this approach the TSM uncertainty propagation method has been chosen to calculate the uncertainties in the efficiency, pressure ratio, corrected mass flow and corrected speed.

It was possible to test the centrifugal compressor at different speeds up to 190 krpm in stable conditions and at 220 krpm with unstable conditions. Testing at 220 krpm was not possible at stable conditions due to the absence of pressure in the system, so the operating points at this speed line could not be measured continuously. Moreover, with these speed-lines the stall and choke limit for the TU Delft compressor were determined.

The uncertainty analysis was used as a tool to study the influence of the different measured variables in the compressor performance map and based on this analysis some suggestions have been given to improve the set-up and measuring system of the test-rig.

The measuring process in the current test-rig can be improved with the change of the pressure sensors, which are the main responsible of the large uncertainty in the efficiency diagrams.

In order to achieve more stable conditions, especially for higher speeds, we should use a larger reservoir tanksuch that the pressurized air that comes into the system would be available for longer time during testing.

It is recommended to implement a heater in the inlet station of the turbine, in this way it can energize the incoming flow and generate more power in the turbine to move the compressor. Furthermore, it should be enhanced the insulation in the piping system.

SYMBOLS

$B_{\bar{x}}$	Expanded bias uncertainty (g/s)
$b_{\bar{x}}$	Elemental bias uncertainty
$B_{\bar{x}\bar{i}}$	Expanded bias uncertainty at inlet (0K)
$b_{\bar{x}i}$	Elemental bias uncertainty at inlet
$B_{\overline{x\bar{o}}}$	Expanded bias uncertainty at outlet (0K)
$b_{\overline{x\bar{o}}}$	Elemental bias uncertainty at outlet
$S_{\bar{x}}$	Expanded random uncertainty
$s_{\bar{x}}$	Elemental random uncertainty
UMF	Uncertainty magnification factor
UPC	Uncertainty percentage contribution
$\dot{m}$	Mass Flow (kg/s)

REFERENCES

[1] "Catalog of Pressure Sensor AE-SML-10", Ae sensors, 2005.

[2] "Data Sheet for Flowmeter Steel Mass Model 640S", Sierra Instruments, 2009.

[3] "Ni cDAQ 9172 User's Manual", National Instruments, NI Press, Austin, TX, 2010.

[4] "Ni9201, Ni9203, Ni9265, Ni 9211 User'sManuals", National Instruments, NI Press, Austin, TX, 2010.

[5] "Product Data Industrial Mineral Insulated Thermocouples, fitted miniature plug, Type K", Lab. Facility temperature and process technology.

[6] "Revised Thermocouple Reference Tables Type K", N.I.S.T, Monograph 175, Revised to ITS-90.

[7] "Test Uncertainty ASME PTC 19.1", ASME, 2005.

[8] "User's guide for Pico Turn-2G", ACAM Mess Electronic.

[9] H.W.Coleman, W.G.Steele,"Experimentation and uncertainty analysis for engineers", 3rd. ed., Ed. New York: John Wiley & Sons Press.,2009

[10] J. Buijtenen, W. Visser, "Thermodynamics and Gas Turbines, AE3-235", Third edition, TU Delft, 2007.

[11] Thermocouple Accuracy Table by Type and Temperature, Internet: http://digital.ni.com/public.nsf/allkb/776AB03E065228408625727B00034E20?OpenDocument, National Instruments.

[12] W.Visser, S.Shakariyants, "Development of a 3 kW Microturbine for CHP Applications", Journal of Engineering for Gas Turbines and Power, Vol. 133.